SNAT3-mediated glutamine transport in perisynaptic astrocytes *in situ* is regulated by intracellular sodium

SCHOLARONE™
Manuscripts

SNAT3-mediated glutamine transport in perisynaptic astrocytes *in situ* is regulated by intracellular sodium

Alison C. Todd[1,2,5], Mari-Carmen Marx[3,5], Sarah R. Hulme[1], Stefan Bröer[4] and Brian Billups[1]

[1]Eccles Institute of Neuroscience, The John Curtin School of Medical Research, The Australian National University, 131 Garran Road, Canberra, ACT 2601, Australia.
[2]School of Biomedical Sciences, University of Edinburgh, Edinburgh, EH8 9XD, UK.
[3]Department of Pharmacology, University of Cambridge, Tennis Court Road, Cambridge CB2 1BT, UK.
[4]Research School of Biology, The Australian National University, Linnaeus Way 134, Canberra, ACT 2601, Australia.

[5]These authors contributed equally to the manuscript

Running Title: Glutamine Transport in Perisynaptic Astrocytes

Word Counts:
           Total Words – 12049
           Abstract - 242
           Introduction - 1073
           Materials and Methods - 1099
           Results - 3009
           Discussion – 2179
           Acknowledgements – 20
           Bibliography – 2440
           Figure Legends – 1987
Number of figures: 12

Main Points:

- Astrocytes *in situ* transport glutamine via the SNAT3 transporter
- EAAT activation causes a rise in $[Na^+]_i$ which alters the SNAT3 equilibrium to release glutamine
- This links neuronal activity to the supply of a neurotransmitter precursor from glia

Address for Correspondence:
     Dr Brian Billups
     Eccles Institute of Neuroscience
     The John Curtin School of Medical Research
     The Australian National University
     131 Garran Road
     Canberra, ACT 2601
     Australia.
     e-mail: brian.billups@anu.edu.au   Tel: +61 2 61252039

Keywords (85 chars): Slc38a3, system N, system A, calyx of Held, EAAT

1

Abstract

The release of glutamine from astrocytes adjacent to synapses in the central nervous system is thought to play a vital role in the mechanism of glutamate recycling and is therefore important for maintaining excitatory neurotransmission. Here we investigate the nature of astrocytic membrane transport of glutamine in rat brainstem slices, using electrophysiological recording and fluorescent imaging of pH_i and Na^+_i. Glutamine application to perisynaptic astrocytes induced a membrane current, caused by activation of system A (SA) family transporters. A significant electroneutral component was also observed, which was mediated by the system N (SN) family transporters. This response was stimulated by glutamine (K_M of 1.57 mM), histidine and asparagine, but not by leucine or serine, indicating activation of the SNAT3 isoform of SN. We hypothesised that increasing the $[Na^+]_i$ would alter the SNAT3 transporter equilibrium, thereby stimulating glutamine release. In support of this hypothesis we show that SNAT3 transport can be driven by changing cation concentration and that manipulations to raise $[Na^+]_i$ (activation of excitatory amino acid transporters (EAATs), SA transporters or AMPA receptors) all directly influence SNAT3 transport rate. A kinetic model of glutamine fluxes is presented, which shows that EAAT activation causes the release of glutamine, driven mainly by the increased $[Na^+]_i$. These data demonstrate that SNAT3 is functionally active in perisynaptic astrocytes *in situ.* As a result, astrocytic Na^+_i signalling, as would be stimulated by neighbouring synaptic activity, has the capacity to stimulate astrocytic glutamine release to support glutamate recycling.

(242 words)

Introduction

Grey matter astrocytes are located in very close proximity to pre- and postsynaptic structures, forming a tripartite synapse (Perea et al. 2009). In line with this concept, astrocytes can sense local levels of neural activity by responding to neurotransmitters, and in turn release substances that modulate synapses. One such released substance is the neutral amino acid glutamine, which does not have a direct neurotransmitter action but is thought to play an important role in supporting neuronal function by contributing to the glutamate-glutamine cycle (see reviews by: Bak et al. 2006; Daikhin and Yudkoff 2000; Hertz et al. 1999; Rothman et al. 2003). According to this hypothesis, synaptically released glutamate is sequestered into neighbouring astrocytes by excitatory amino acid transporters (EAATs), and is then converted to glutamine by the astrocytic enzyme glutamine synthetase (GS). This glutamine is subsequently transported out of astrocytes and into neurons, where it is used to re-synthesise glutamate for continued neurotransmission. In support of this hypothesis, recent evidence has demonstrated that extracellular glutamine is required for sustaining maximal levels of excitatory synaptic transmission (Billups et al. 2013; Marx et al. 2015; Rae et al. 2003; Tani et al. 2014). Astrocytes are implicated as the source of this glutamine since GS, the main glutamine-producing enzyme, is located exclusively in glia and is abundant in astrocytes (Norenberg and Martinez-Hernandez 1979). Inhibition of GS with methionine sulfoximine (MSO) results in reduced levels of glutamatergic transmission (Tani et al. 2014), reduced tissue glutamine content in the neocortex (Tani et al. 2010) and reduced glutamine levels in cultured hippocampal astrocytes (Laake et al. 1995). As presynaptic glutamate is the main precursor for neuronal GABA, glutamine derived from astrocytes may also be important for producing presynaptic GABA (Sonnewald et al. 1993) and maintaining the function of GABAergic synapses (Fricke et al. 2007; Jiang et al. 2012; Liang et al. 2006; Yang and Cox 2011).

The mechanism of glutamine release from astrocytes at synapses is uncertain, but likely to be mediated by a specific neutral amino acid transporter. Several families of such transporters have been localised to astrocytes including members of systems L, y^+L, ASC, A and N (Deitmer et al. 2003; Dolinska et al. 2004; Heckel et al. 2003; Nagaraja and Brookes 1996; Sidoryk-Wegrzynowicz et al. 2009). While these transporters are all capable of transporting glutamine, some (L, y^+L and ASC) are thought to be exchangers (Broer et al. 1999; Broer et al. 2000; Pineda et al. 1999), which can only release significant glutamine by sequestering another amino acid, and are therefore not responsible for the net amino acid efflux required for neurotransmitter recycling. Contrary to the exchangers, system A (SA)

3

and system N (SN) transporters catalyse flux of only one amino acid per transport cycle and have the capacity to alter the total amino acid content of the astrocyte. SA mediated glutamine transport is electrogenic, being coupled to the co-transport of one Na^+ (Chaudhry et al. 2002), and is consequently only capable of mediating net glutamine influx at the negative membrane potentials of astrocytes. In contrast, SN glutamine transport is thought to be coupled to a co-transported Na^+ and an additional counter-transported H^+, resulting in an electroneutral transport mechanism that is bidirectional under physiological conditions (Broer et al. 2002; Chaudhry et al. 2001; Chaudhry et al. 1999). This suggests that SN mediated transport is a potential mechanism for astrocytic glutamine efflux as part of the glutamate-glutamine cycle.

The main SN transporter family members are SNAT3 and SNAT5, which arise from the genes *Slc38a3* and *Slc38a5*, and are also known as SN1 and SN2 respectively (Broer 2014). SNAT7 (*Slc38a7*) also demonstrates some SN characteristics and may be an additional member of this transporter system (Hagglund et al. 2011). SNAT3 transports mainly glutamine, histidine and asparagine (Chaudhry et al. 1999; Gu et al. 2000) and its expression in the brain is exclusively glial, being most concentrated in astrocytic processes surrounding neurons (Boulland et al. 2002; Boulland et al. 2003). SNAT5 is also localised to astrocytes (Cubelos et al. 2005) but has broader substrate specificity, additionally transporting serine, alanine and glycine (Hamdani el et al. 2012; Nakanishi et al. 2001a; Nakanishi et al. 2001b). Both SNAT3 and SNAT5 induce pH changes in cells by virtue of the counter-transported H^+, and both are able to efficiently transport glutamine using either Na^+ or Li^+ as the co-transported cation (Chaudhry et al. 1999; Gu et al. 2000; Nakanishi et al. 2001a) which is a characteristic property of SN (Taylor et al. 1992). The first aim of our study was to identify the nature of the glutamine transport in perisynaptic astrocyte *in situ*. The pharmacology of SA/SN transporters is ill developed, as a result we used a combination of ion selectivity and substrate specificity to identify the relevant transporters. We show that a component of astrocytic glutamine transport has the properties of SNAT3, but we do not observe SNAT5 mediated transport.

We investigated glutamine transporter function in astrocytes in the rat medial nucleus of the trapezoid body (MNTB). This region of the auditory brainstem receives input from the contralateral cochlea nucleus via the calyx of Held synapse onto the principal cells of the MNTB (Smith et al. 1998). The calyx of Held is a large glutamatergic synapse that is easily identifiable in acute brain slices using light microscopy, and is ideal for comprehensively

4

investigating synaptic transmission in living neuronal tissue (Schneggenburger and Forsythe 2006). Astrocytes are located immediately adjacent to this synapse, which can be easily identified and patch-clamped (Muller et al. 2009; Reyes-Haro et al. 2010; Uwechue et al. 2012). The close proximity of the astrocytic somata to the active synapses permits recording from a defined population of glial cells that are likely to be involved in the glutamate-glutamine cycle. Using this preparation we have previously shown that activating excitatory amino acid transporters (EAATs) on astrocytes, as would occur during synaptic transmission, causes them to rapidly release glutamine within a few milliseconds (Uwechue et al. 2012). We hypothesised that this astrocytic glutamine release is mediated by SNAT3 and is triggered by the EAAT-induced rise of intracellular sodium concentration ($[Na^+]_i$) (Kirischuk et al. 2016). Consequently, in this study we investigated the ability of cations to activate SNAT3. We show that astrocytic SNAT3 glutamine transport is controlled by transmembrane $[Na^+]$, and is regulated by EAAT activity. This demonstrates a mechanism by which synaptic activity can induce astrocytic glutamine release, which could then be sequestered by presynaptic terminals for subsequent replenishment of neuronal glutamate.

Materials and Methods

Slice Preparation

Wistar rats (male and female), 10 to 17 days old, were killed by decapitation, in accordance with procedures approved by the Animal Experimentation Ethics Committee of the Australian National University and in compliance with the UK Animal (Scientific Procedures) Act 1986. Brains were swiftly removed and transferred to oxygenated ice cold slicing solution containing (in mM): 2.5 KCl, 10 HEPES, 1.25 NaH_2PO_4, 10 glucose, 290 sucrose, 4 $MgCl_2$, 0.1 $CaCl_2$, and pH set to 7.3 with NaOH. Transverse brain slices, 100 – 140 μm thick, of the auditory brainstem containing the MNTB were made using an Integraslice 7550 PSDS tissue slicer (Campden Instruments). Slices were placed in an incubation chamber at 37 ^{0}C for 30 minutes containing O_2 bubbled artificial cerebrospinal fluid (aCSF) composed of (in mM): 145 NaCl, 2.5 KCl, 10 HEPES, 1.25 NaH_2PO_4, 10 glucose, 1 $MgCl_2$, 2 $CaCl_2$, with osmolarity of 320 mmolkg^{-1} and pH set to 7.3 with ~4.5 mM NaOH. Following incubation, the chamber and slices were left to rest in aCSF at room temperature and used within 8 hours.

Electrophysiological Recording

Patch-clamp electrode and puffer pipettes were pulled from thick-walled borosilicate glass capillaries (GC150F-7.5; Harvard Apparatus). Electrodes for astrocyte recordings had open tip resistance of 6 – 6.5 MΩ and were filled with internal solution containing (in mM): 130 KCl, 4 Glucose, 20 Sucrose, 10 HEPES, 0.1 EGTA, 0.025 $CaCl_2$, 1.4 MgATP, 0.6 NaGTP, pH set to 7.2 by KOH and osmolarity made up to 305 mmolkg^{-1} by the addition of sucrose. For 15 mM $[Na^+]_i$ internal solution, the 20 mM sucrose was replaced by 14.4 mM NaCl. During recording brain slices were continually perfused with aCSF (composition as above) at 22.2 – 25.5^{0}C, at a rate of 1 ml min^{-1}, and visualised with infrared differential interference contrast (DIC) optics. Astrocytes located adjacent to characteristically large spherical principal cells of the MNTB were whole-cell patch-clamped, and membrane currents were recorded with astrocytes voltage-clamped at -80 mV using a HEKA EPC-10 double amplifier, low-pass filtered at 10 and 2.9 kHz, and digitized at 25 kHz with Patchmaster software (HEKA). Cell identification was confirmed by fluorescent imaging of intracellular dyes and by electrophysiological properties (membrane resistance <10 MΩ; resting membrane potential more negative than -75 mV; lack of voltage-activated currents; approximately linear current-voltage relationship). All chemicals were purchased from Sigma-Aldrich, except APV, bicuculline, MK-801, NBQX (Abcam); TTX (Latoxan); TFB-TBOA (Tocris) and sodium-binding benzofuran isophthalate tetraammonium salt (SBFI; Invitrogen).

6

Fluorescent Na$^+$ and pH Imaging

For fluorescent imaging, individual astrocytes were whole-cell patch-clamped using intracellular solution with the addition of 250 μM 8-Hydroxypyrene-1,3,6-trisulfonic acid (HPTS) for pH imaging or 250 μM SBFI for Na$^+$ imaging. Cells were illuminated using a monochromator (Optoscan, Cairn Research), visualised with a 60X N.A. 1.0 fluorite water-immersion lens (Nikon) and imaged with 100 ms exposure times at 1 frame per second using an electron-multiplying CCD camera (Cascade 512B, Photometrics) controlled by MetaFluor software (Molecular Devices). For pH imaging, HPTS was excited at 465 and 405 nm; emitted light was separated with a 505 nm dichroic mirror and collected via a 520 nm long pass filter (Nikon B-2A). The light collected with 465 and 405 nm excitation was background subtracted and 465:405 ratio used to indicate pH (Willoughby et al. 1998). For Na$^+$ imaging, SBFI was excited at 385 and 350 nm; emitted light was separated with a 400 nm dichroic mirror and collected via a 420 nm long pass filter (Nikon UV-2A). The light collected with 350 and 385 nm excitation was background subtracted and 350:385 ratio used to indicate [Na$^+$]$_i$ (Minta and Tsien 1989). Approximate calibration of both pH$_i$ and [Na$^+$]$_i$ was performed by construction of a linear calibration curve using pipette solutions of known pH (pH 6.8 to 8.6) and [Na$^+$]$_i$ (0 to 10 mM) respectively.

For activation of astrocytic transporters, substrates were either bath-applied or pressure-ejected from adjacent pipettes (Picospritzer III). Puffer pipettes (tip diameter ~2 μm) were filled with aCSF with the addition of experimental substrates and placed 50 to 80 μm from the patch-clamped astrocyte. For comparison between substrates (Fig. 4), substrates were applied in an alternating fashion from two puffer pipettes, pulled from the same capillary and placed equidistant from the cell. For Na$^+$ replacement aCSF, NaCl was replaced with either NMDG-Cl (pH balanced with NMDG) or LiCl (pH balanced with LiOH), as required. NaH$_2$PO$_4$ was also replaced with KH$_2$PO$_4$, and 1.25 mM of KCl substituted by LiCl to maintain a constant K$^+$ concentration. Replacement aCSF was washed-on for > 20 minutes to ensure thorough cation exchange before recording data.

Transporter flux modelling

To estimate the fluxes associated with SN activation a model was used to calculate the transporter generated flux based on the concentrations of the transported substrates and their apparent affinities for the transporter, using the following equation (Equation 1):

$$J_{SN} = \mathrm{P}\left[\left(\frac{Gln_o}{K_{M(Gln)}+Gln_o} * \frac{H_i^+}{K_{M(H)}+H_i^+} * \frac{Na_o^+}{K_{M(Na)}+Na_o^+}\right) - \left(\frac{Gln_i}{K_{M(Gln)}+Gln_i} * \frac{H_o^+}{K_{M(H)}+H_o^+} * \frac{Na_i^+}{K_{M(Na)}+Na_i^+}\right)\right]$$

Where J_{SN} is the transporter flux (positive values indicate glutamine influx; negative values indicate efflux), P the maximum permeability of molecules through all the transporters in the cell, and $K_{M(Gln)}$, $K_{M(H)}$ and $K_{M(Na)}$ represent the apparent affinities for glutamine, H^+ and Na^+ respectively. $K_{M(Gln)}$ was set to 1.57 mM (see Results, Fig 2B.), $K_{M(H)}$ to 100 nM (i.e. $pK_{M(H)}$ = 7.0) and $K_{M(Na)}$ to 31 mM (Broer et al. 2002). The relationship between H^+ flux and ΔpH_i was determined by $\Delta pH_i = \beta * 10^{\wedge}(-\Delta[H^+]_i)$; where β represents an intracellular buffering effect. β was determined to be 107,218 by comparing the observed ΔpH_i to $\Delta[Na^+]_i$ upon SN activation (see Results Fig. 2E, G), assuming a 1:1 stoichiometry for $Na^+:H^+$ transport by SN. Following glutamine application, pH_i and $[Na^+]_i$ are observed to return to baseline levels over 30 to 60 s, by unknown mechanisms assumed to be a combination of diffusion, buffering and compensatory transport. This was implemented in the model by adding decay rates for H^+_i and Na^+_i of 0.1 s^{-1} to match the observed data. Using Equation 1, β and the decay rates, SN flux and intracellular concentration changes were calculated over time, assuming constant extracellular concentrations. To achieve this, an iterative function was used with time steps of 100 ms, which was implemented using Excel. To calculate changes in internal concentrations from fluxes, a cell volume of 0.065 pl and surface area of 7.85 x 10^{-11} m^2 were assumed (i.e. a spherical cell of 5 µm diameter).

Data Analysis

Results are presented as mean ± SEM. Statistical comparisons were performed using paired 2-tailed t-tests assuming equal variances (Excel). For multiple comparisons (Figs. 1D, 2F, 3E, 4G, 7B, 7D, 8B and 8D), linear mixed effect model (LME) ANOVA was used, in consultation with the Statistical Consulting Unit, Australian National University, and implemented in R.

Results

To investigate the presence of functional system N (SN) transporters on astrocytic membranes *in situ*, astrocytes in acutely isolated rat brainstem slices were whole-cell voltage-clamped to measure their membrane currents. Fluorescent ion indicators were also included in the patch pipette to simultaneously measure the ion changes associated with activation of membrane transporters. Recorded astrocytes were located adjacent to the cell bodies of the principal neurons of the MNTB (Fig. 1A), as these glia are known to be in close association with the calyx of Held glutamatergic presynaptic terminal (Rowland et al. 2000; Satzler et al. 2002). Membrane transporters were activated by puff-application of transporter substrates from one of two puffer pipettes positioned 20 - 50 μm away from the astrocyte (Fig. 1A). Voltage-clamp recordings were confirmed to be from astrocytes as they displayed no voltage activated currents, exhibited a resting membrane potential of -80.8 ± 0.2 mV and had a membrane resistance of 2.9 ± 0.3 MΩ (Fig. 1B; n = 167).

System N and System A Activation in Perisynaptic Astrocytes

Puff application of 10 mM glutamine to activate astrocytic glutamine transporters induced a membrane current (I_{Gln}) of -20.0 ± 2.4 pA (n = 27), which was almost entirely eliminated by the substitution of Na^+ in the external solution with Li^+ (Fig. 1C): I_{Gln} was reduced 94 ± 5 % by Li^+ substitution (Fig. 1D; n = 6, P = 0.01). As SN transport is known to be tolerant of such Li^+ substitution, this result indicates that the vast majority of glutamine induced membrane current is not mediated by SN. It has previously been shown that some astrocytes may express electrogenic SA glutamine transporters. Hence, SA activation may have been responsible for producing the observed glutamine induced currents. To test this hypothesis, a saturating concentration of the SA substrate α-(Methylamino)isobutyric acid (MeAIB) was added to the external solution. MeAIB binds to SA but is transported more slowly than glutamine (Chaudhry et al. 2002), so when used in excess it acts to occlude further SA activity, without directly inhibiting SN (Chaudhry et al. 2001). In the presence of 20 mM MeAIB, I_{Gln} was reduced 92 ± 5% (Fig. 1D; n = 4, P < 0.01), indicating that the majority of I_{Gln} is mediated by an MeAIB sensitive transporter, which is likely to be SA.

As SN transport does not mediate the vast majority of I_{Gln}, its main mode of operation is likely to be electroneutral. As an alternative to assessing the membrane current, SN transport activity can be studied by measuring the ion concentration changes resulting from

the counter transport of H^+ or co-transport of Na^+. Consistent with this stoichiometry, imaging with the ratiometric pH indicator, HPTS, included in the patch-pipette revealed an astrocytic alkalinisation induced by application of glutamine. Increasing concentrations of glutamine added to the bath perfusion resulted in progressively larger astrocytic alkalinisation, with 20 mM producing a change of approximately 0.2 pH units (Fig. 2A). This dose-response is fit by a Michaelis-Menten relationship with a K_m of 1.57 mM (Fig. 2B). Puff application of glutamine (10 mM for 5 s) produced an average astrocytic pH change of 0.062 ± 0.003 pH units (n = 59), while control aCSF puffs containing no glutamine elicited a negligible pH change of 0.004 ± 0.001 pH units (n = 3; Fig. 2C-D). Comparing the pH response to a glutamine puff with the dose-response of bath applied glutamine in the same cell reveals that for a 10 mM glutamine puff, the concentration reaching the cell is equivalent to bath application of 0.86 ± 0.29 mM (n=6).

As commercially supplied glutamine may contain contaminant glutamate (Sands and Barish 1989; Yamada and Rothman 1989), which could activate glutamate receptors or transporters and produce an indirect pH change, the effects of glutamate transporter and ion channel inhibitors was examined. Accordingly, the glutamine induced pH change was unaffected by inhibition of EAAT glutamate transporters with the EAAT antagonist TFB-TBOA (20 µM). The glutamine-induced pH change was 0.058 ± 0.009 pH units in control, and 0.060 ± 0.009 pH units with TFB-TBOA included in the aCSF (n = 5; P = 0.75; Fig. 2E-F). A cocktail of compounds to inhibit ion channels (40 µM APV, 10 µM MK-801, 20 µM NBQX, 1 µM TTX, 1 µM strychnine and 10 µM bicuculline) likewise did not inhibit the pH_i change: the control pH_i change was 0.065 ± 0.019 pH units, and upon addition of the channel inhibitors the pH_i response was 0.077 ± 0.02 pH units, which represents a slight increase in response (n = 4; P = 0.02; Fig. 2F). This rules out the possibility of direct or indirect activation of glutamate receptors/transporters causing the glutamine-induced pH_i change. To investigate the influence of the endogenous astrocytic pH buffering mediated by sodium-bicarbonate exchangers (Theparambil and Deitmer 2015; Theparambil et al. 2015), some experiments were performed in external solution buffered with 26 mM $NaHCO_3$. However, although glutamine induced alkalinisations were similarly observed, significant pH artefacts were recorded when puff-applying only aCSF (Supplementary Fig. 1). To avoid these artefacts HEPES buffered solutions were used throughout.

Glutamine-Induced pH Changes are Mediated by System N

Consistent with the glutamine-induced pH_i change being mediated by a sodium-dependent transport process, intracellular sodium imaging with SBFI showed an increase in $[Na^+]_i$ in response to puff-application of 10 mM glutamine (Fig. 2G). The magnitude of the $[Na^+]_i$ rise was 0.90 ± 0.07 mM (n = 12) in the astrocytic soma and, as with the pH changes, this was unaffected by EAAT inhibition with TFB-TBOA (0.89 ± 0.17 mM and 0.95 ± 0.14 mM for control and TFB-TBOA respectively; n = 4; P = 0.70; Fig. 2G-H). Taken together, these results are consistent with the activation of a glutamine transporter in the astrocytic membrane that is coupled to the co-transport of Na^+ and the counter-transport of H^+.

As expected for a sodium-dependent transporter mediated response, removal of the extracellular Na^+ and replacement with NMDG completely inhibited the pH_i change: the pH_i change in control solution (0.065 ± 0.006 pH units) was reduced 96% by the removal of Na^+ (0.002 ± 0.001 pH units; n = 4; P < 0.0001; Fig. 3A, E). SN is unique amongst sodium-dependent transporters in its ability to maintain its transport rate when Li^+ is substituted for Na^+. We therefore tested the effects of glutamine application in Li^+ solution. Replacement of Na^+ with Li^+ did not affect the glutamine induced pH_i change (0.050 ± 0.006 and 0.050 ± 0.005 pH units for Na^+ and Li^+ solutions respectively, n = 12; P = 0.82; Fig. 3B, E). Over a period of 30 minutes, the response in Li^+ solution remained stable (Fig. 3D), unlike the decline in the response seen with NMDG solution (which demonstrates the time course of removing the transported cation from the brain slice).

Sodium-dependent glutamine transporters such as SN and SA can also accept histidine as an amino acid substrate, whereas the sodium-independent amino acid transport system, system L, does not transport histidine but does accept leucine. Adding histidine or leucine to the bath to saturate amino acid binding sites therefore provides information about the type of amino acid transporter mediating the observed pH changes. In the presence of 20 mM histidine, the glutamine-induced pH_i change was totally occluded, being reduced by 99% from 0.058 ± 0.006 to 0.001 ± 0.001 pH units (n = 7; P < 0.0001; Fig. 3C, E). In contrast, in the presence of 20 mM leucine the pH_i response to glutamine puffs was unchanged (0.053 ± 0.007 and 0.055 ± 0.006 pH units in control and leucine respectively; n = 4; P = 0.48; Fig. 3E).

Substrate Profile of System N

11

Identification of the amino acid transporter responsible for the glutamine-induced pH_i response is aided by exploring the substrate profile. To investigate this, two puffer pipettes were used to alternately apply 10 mM glutamine or 10 mM of another amino acid to the astrocyte. The rate of amino acid transport relative to the rate of glutamine transport was then assessed. Compared to glutamine, puffs of histidine produced an alkalinisation of 76 ± 12 % (n = 4; P < 0.005 compared to aCSF; Fig. 4A, G) and asparagine an alkalinisation of 41 ± 9 % (n = 6; P = 0.05 compared to aCSF; Fig. 4B, G). Alanine, which is a weak SN substrate, consistently produced a small response (24 ± 6 % of the glutamine response; n = 7; Fig. 4C, G), although this was not significantly different from control aCSF puffs (P = 0.22). Serine (a system ASC substrate), leucine (a system L substrate) and MeAIB (a system A substrate) did not produce a pH_i response when puff-applied to astrocytes (n = 7, 5 and 8 respectively; P = 0.97, 0.94 and 0.89; Fig. 4D-G). This amino acid substrate profile, along with the electroneutrality, sodium-dependence and lithium-tolerance, identifies the activated transporter system as system N.

System N Activation by Cations

While we have demonstrated that glutamine transport can be activated by increasing the glutamine concentration in the presence of a co-transported cation (Na^+ or Li^+; Fig. 3A, B), we have previously proposed that, under physiological conditions, glutamine release via SN transport is activated by an increase in cation concentration in the continued presence of glutamine (Uwechue et al. 2012). To test this hypothesis, rather than applying Na^+ to astrocytes, which would influence many transporters and ion channels, we applied Li^+ and recorded the resulting glutamine transport-mediated pH_i change. Bathing astrocytes in a solution containing 20 mM Li^+ (balanced with 126 mM $NMDG^+$), and puff applying 150 mM Li^+ produced no astrocytic pH_i change when glutamine was omitted from the solution. However, in the presence of 20 mM glutamine, Li^+ puffs induced a pH_i change of 0.009 ± 0 0.002 pH units (n = 4; P = 0.045; Fig. 5A, B). This demonstrates that astrocytic glutamine transport is capable of being driven by increases in cation concentration in the continued presence of glutamine.

Astrocytic Intracellular Sodium Signals

It follows that if changes in cation concentration can influence SN transport rate, then cellular processes that increase $[Na^+]_i$ would be expected to activate SN and cause glutamine efflux. For example, transport of glutamate into astrocytes by EAATs would increase $[Na^+]_i$, which

could drive glutamine efflux. While stimulation of glutamine efflux by EAAT activation has been previously shown (Martinez-Lozada et al. 2013; Uwechue et al. 2012) the link via $[Na^+]_i$ has not been demonstrated. To investigate this link, we performed three different manipulations to increase the $[Na^+]_i$.

First, astrocytic EAATs were activated by the EAAT substrate D-aspartate. Puff application of 200 µM D-aspartate resulted in an inward EAAT current (-51 ± 5 pA; n = 4), which was blocked when the EAAT inhibitor TFB-TBOA (20 µM) was added to the bathing solution (current reduced to -1 ± 1 pA; n = 4; P = 0.002; Fig. 6A, C). Amino acid transport by EAATs is driven by the co-transport of 3 Na^+ ions, and hence EAAT activation by D-aspartate is accompanied by a rise in $[Na^+]_i$. Increases of $[Na^+]_i$ were measured by including SBFI in the patch pipette, and a change of 0.84 ± 0.16 mM (n = 4) was observed following 200 µM D-aspartate puffs (Fig. 6B, C). As was observed for the EAAT current, the EAAT-induced increase in $[Na^+]_i$ was eliminated by 20 µM TFB-TBOA (0.004 ± 0.03 mM; n = 4; P = 0.02; Fig. 6C). Similarly, bath application of 200 µM D-aspartate also resulted in a $[Na^+]_i$ rise (2.3 ± 0.5 mM; n = 3; Fig. 6D).

The second method used to increase $[Na^+]_i$ was to activate astrocytic SA transporters by bath application of 20 mM MeAIB, since SA co-transports a Na^+ ion with its substrate. As anticipated, this caused an increase of $[Na^+]_i$ (0.98 ± 0.27 mM; n = 4; Fig. 6E). The final method used to increase $[Na^+]_i$ was to activate astrocytic AMPA receptors (AMPARs) using the ionotropic glutamate receptor agonist kainate. Kainate was used as an AMPAR agonist as it does not cause the rapid desensitization observed following activation by glutamate (Patneau and Mayer 1990). We observed that bath application of 300 µM kainate caused an increase in $[Na^+]_i$ of 9.1 ± 0.7 mM (n = 3; Fig. 6F).

Changes in $[Na^+]_i$ Influence Glutamine Transport

We hypothesise that each of the manipulations used to raise astrocytic $[Na^+]_i$ would consequently cause glutamine efflux by activation of SN. To demonstrate this, we activated SN mediated glutamine influx by puff application of glutamine to the external astrocytic membrane and measured the resultant pH_i change. We consistently observed a reduction of this influx when $[Na^+]_i$ was increased, implying that in the raised $[Na^+]_i$ condition the transporter's efflux/influx equilibrium was shifted towards net glutamine efflux under basal conditions. Increasing $[Na^+]_i$ by activation of EAATs with bath-application of 200 µM D-

13

aspartate caused a reduction in the glutamine-induced pH_i change (to 58 ± 6 % of control; n = 4; P = 0.0005; Fig. 7A, B). This effect was blocked by the addition of the EAAT inhibitor TFB-TBOA to the recording medium, with the glutamine induced pH change being 106 ± 4 % of control (n = 3, P = 0.70; Fig. 7B). As the intracellular patch-pipette solution contained a negligible amount of Na^+, this experiment was repeated with $[Na^+]_i$ = 15 mM, to reflect the physiological levels of astrocytic $[Na^+]_i$ (Rose and Ransom 1996; Unichenko et al. 2012) and to more accurately mimic the expected changes in $[Na^+]_i$ upon EAAT activation. Under these conditions, 200 µM D-aspartate caused a similar reduction in the glutamine-induced pH_i change to 67 ± 8 % of control; n = 4; P < 0.0001; Fig. 7C, D). Averaged data showing the time-dependence of the D-Aspartate effect is shown in Fig. 7E.

Similar to raising $[Na^+]_i$ by EAAT activation, increasing $[Na^+]_i$ by activation of SA transporters with bath-application of 20 mM MeAIB caused a reduction in the glutamine-induced pH_i change to 68 ± 5 % of control (n = 10; P < 0.0001; Fig. 8A, B). Finally, increasing $[Na^+]_i$ by activation of AMPARs with 300 µM kainate also caused a reduction in the glutamine-induced pH change (to 75 ± 5 % of control; n = 4; P = 0.002; Fig. 8C, D). This effect of kainate was blocked by the addition of 20 µM NBQX, a specific AMPA/kainate receptor antagonist, to the recording medium (response in kainate/NBQX was 94 ± 2 % of control; n = 3; P = 0.55; Fig. 8D). The time-dependent effect to the SN inhibition due to kainate application, and its lack of effect in NBQX, are shown in Fig. 8E. These three independent methods of increasing $[Na^+]_i$ and the resultant decrease in SN glutamine influx all support our hypothesis that raised $[Na^+]_i$ causes efflux of glutamine via SN in perisynaptic astrocytes.

Modelling of System N Mediated Glutamine Efflux

To mathematically model transporter function and demonstrate the ability of SNAT3 to function in a bidirectional manner under physiological conditions, transporter fluxes were calculated according to Equation 1 (see methods). Using concentrations from our experimental conditions (0 mM glutamine, $[Na^+]$ and pH from the external and internal solutions), the effect of increasing the extracellular glutamine to 0.86 mM for 5 s (equivalent to a 10 mM puff application) could be observed (Fig. 9A). To produce a pH_i and $[Na^+]_i$ change identical to the observed data, an optimal value for P of 1.755 $\mu mol.m^{-2}.s^{-1}$ was determined by least-squared calculation. This constant is proportional to the maximal rate of each SNAT3 transporter and the total number of transporters present in the astrocyte.

14

Using these calculated parameters, we then probed the model to determine the effect of activating astrocytic EAAT transporters on SNAT3 mediated glutamine fluxes. First, we set-up an equilibrium condition for the astrocyte at rest where J_{SN} = 0. This was achieved with pH_o = 7.3, pH_i = 7.2, $[Na^+]_o$ = 152 mM, $[Na^+]_i$ = 15 mM (Rose and Ransom 1996; Unichenko et al. 2012) and $[Gln]_o$ = 0.5 mM (Jacobson et al. 1985; Kanamori and Ross 2004; Reichel et al. 1995). From Equation 1, zero-flux equilibrium would be achieved when $[Gln]_i$ = 3.8992 mM, which is consistent with experimentally observed low mM values of $[Gln]_i$ in astrocytes (Ottersen et al. 1992; Patel and Hunt 1985; Schousboe et al. 1979). Subsequently, EAAT activation was simulated by adding ion fluxes to the model. EAAT-mediated glutamate transport is electrogenic, being powered by the co-transport of 3 Na^+ and 1 H^+, and the counter-transport of 1 K^+ (Zerangue and Kavanaugh 1996). As SNAT3 transport is electroneutral and K^+ insensitive, changes in $[K^+]_i$ and membrane voltage mediated by EAAT activation were ignored. EAAT activation was thus simulated by adding a Na^+ influx to give a $\Delta[Na^+]_i$ of 10mM (Bennay et al. 2008; Kirischuk et al. 2007; Langer and Rose 2009), and H^+ influx was set to Na^+ influx / 3. Under these conditions a Na^+-stimulated glutamine efflux is observed that persists for 20 s (Fig. 9B).

In our experiments we activated EAATs with D-aspartate, which is not a substrate for GS and therefore will not produce glutamine inside astrocytes. However, physiologically, EAAT-mediated transport of glutamate will increase $[Gln]_i$ via the action of GS. Up to 50% of the sequestered glutamate is known to be metabolised by the TCA cycle and we assume that the remainder is converted to glutamine (McKenna 2007). To investigate how this added Gln_i would influence the SNAT3 flux following EAAT activation, $[Gln]_i$ was increased in the model following EAAT activation, assuming instantaneous conversion of glutamate to glutamine. This increase in $[Gln]_i$ resulted in an enhancement of glutamine efflux, by a factor of 2.4 (Fig. 9C). However, this greater glutamine efflux is still driven mainly by the rise in $[Na^+]_i$. If the EAAT induced change in Na^+_i, Gln_i and H^+_i are separately added to the model (Fig. 10), Na^+_i induces a maximal efflux of 45.3 $nmol.m^{-2}.s^{-1}$ (Fig 10A), H^+_i an influx of 31.7 $nmol.m^{-2}.s^{-1}$ (Fig. 10B) and Gln_i an efflux of 14.1 $nmol.m^{-2}.s^{-1}$ (Fig 10C). This demonstrates that the changes in $[Na^+]_i$ are the major driving force for the release of glutamine via SNAT3.

Discussion

In this study we have characterised aspects of glutamine transport in astrocytes *in situ*, which are located immediately adjacent to synapses. We have shown that system N transport is functional in perisynaptic astrocytes and that it is strongly influenced by cellular mechanisms that modulate intracellular $[Na^+]$, most notably activation of EAAT glutamate transporters. This creates a functional link between the influx of glutamate and the efflux of glutamine from astrocytes, which is a key component of the glutamate/glutamine cycle (Fig. 11).

Previous studies of glutamine transport in glia have mainly relied on studying primary astrocyte cultures. These have indicated that systems L, ASC, A and N are the predominant transporters, with the contribution of SN ranging from 10 to 50% of the total glutamine transport capacity (Deitmer et al. 2003; Dolinska et al. 2004; Heckel et al. 2003; Nagaraja and Brookes 1996; Sidoryk-Wegrzynowicz et al. 2009). siRNA knockdown of SN transporters reveals a dominant role for SN in mediating glutamine release from cultured neocortical astrocytes (Zielinska et al. 2016). In comparison, glial derived cell lines express different subsets of glutamine transporters, with ASC rather than SN having the most significant contribution (Dolinska et al. 2004; Heckel et al. 2003; Sidoryk et al. 2006). However, cultured glia are known to express different transporters, receptors and ion channels compared to acutely isolated tissue (Kimelberg et al. 2000), and hence the contribution of SN to astrocytic glutamine transport *in situ* is uncertain. Immunohistochemical studies have localised the SN transporters SNAT3 (Boulland et al. 2002) and SNAT5 (Cubelos et al. 2005) to astrocytic processes located adjacent to glutamatergic and GABAergic synapses, confirming the presence of the protein in native tissue. Our recordings extend this by demonstrating that SN is functionally expressed in the astrocytic plasma membrane.

As glutamine transport by SN is thought to be accompanied by the co-transport of one Na^+ and the counter transport of an H^+ (Broer et al. 2002; Chaudhry et al. 2001; Chaudhry et al. 1999), we assessed SN activity by imaging the intracellular pH changes that result from SN activation. *In situ,* SN would operate at equilibrium unless changes of pH, $[Na^+]_i$ or $[glutamine]_i$ occur, and readily facilitates either glutamine influx or efflux (Broer et al. 2002).

16

By applying glutamine to the external surface of the astrocytic plasma membrane, we have used the glutamine influx mode, and associated intracellular alkalinisation, to demonstrate SN activity in these cells.

The glutamine induced pH change is Na^+-dependent, but of equal magnitude when Li^+ is substituted for Na^+ as the transported cation. Only transport via SN is insensitive to this type of Li^+/Na^+ substitution, which is regarded as a defining feature of this transport system (Chaudhry et al. 1999; Gu et al. 2000; Nakanishi et al. 2001a; Taylor et al. 1992). Although Li^+ can support a degree of transport via some Na^+-dependent transport systems (e.g. system A: Chaudhry et al. 2002; Mackenzie et al. 2003), the rates of transport with Li^+ are greatly reduced compared to Na^+-driven transport. Our observation of a Na^+-dependent transport process that is completely Li^+-insensitive strongly supports the conclusion that the pH_i changes we observe are mediated by SN. In agreement of this conclusion, the transport we observe shows the substrate selectivity of SN (Chaudhry et al. 2001; Chaudhry et al. 1999; Fei et al. 2000; Hamdani el et al. 2012), transporting glutamine, histidine and asparagine, possibly weakly alanine, but not leucine (a system L substrate, Segawa et al. 1999), serine (a system ASCT substrate, Utsunomiya-Tate et al. 1996) or MeAIB (a system A substrate, Chaudhry et al. 2002). Furthermore, the affinity for glutamine we record is 1.6 mM, which is consistent with the range of glutamine affinities recorded for SN (1.0 to 2.4 mM; Baird et al. 2004; Broer et al. 2002; Chaudhry et al. 2001; Chaudhry et al. 1999; Fei et al. 2000; Gu et al. 2000; Hamdani el et al. 2012), but significantly different to the glutamine affinities of system L (isoform LAT2: 151 – 316 μM, Rajan et al. 2000; Segawa et al. 1999), y^+L (isoform y^+LAT2: 296 μM, Broer et al. 2000) and ASC (isoform ASCT2: 24 – 70 μM, Broer et al. 1999; Utsunomiya-Tate et al. 1996).

The two main SN isoforms, SNAT3 and SNAT5, are both expressed in astrocytes and could contribute to the observed transport activity. SNAT3 and SNAT5 have similar properties regarding their stoichiometry and Li^+-tolerance, however SNAT5 can facilitate the transport of a great number of substrates, including serine (Hamdani el et al. 2012; Nakanishi et al. 2001a). Although serine is a much more effective SNAT5 substrate than glutamine, we did not observe astrocytic SN activity in response to serine application. The relative magnitudes of transport of glutamine, histidine, asparagine, alanine and serine are entirely consistent with the observed substrate profile of SNAT3 and inconsistent with the presence of any SNAT5. This indicates that SNAT3 is the only SN transporter that is functionally expressed on the plasma membrane of these astrocytes. The lack of functional SNAT5 could be due to

17

the intracellular localisation of SNAT5 compared to SNAT3 (Hamdani el et al. 2012), regional differences in expression between the two transporters (Boulland et al. 2002; Cubelos et al. 2005) or developmental regulation of SNAT5 expression (Rodriguez et al. 2014). As the recently proposed SN family member SNAT7 does not facilitate transport when Li^+ replaces Na^+ (Hagglund et al. 2011), the glutamine transport we observe is not mediated by SNAT7.

In addition to SN mediated pH_i changes, glutamine induced a sodium-dependent, MeAIB-sensitive membrane current in astrocytes, which can be ascribed to activation of SA. SA-mediated glutamine transport in astrocytes has previously been investigated in primary culture, with some groups reporting a low level of expression compared to neurons (Dolinska et al. 2004), activity mainly in response to nutrient deprivation (Nagaraja and Brookes 1996), or no activity at all (Heckel et al. 2003). However, mRNA for the SA isoform SNAT2 is expressed in cultured astrocytes (Dolinska et al. 2004; Heckel et al. 2003) and immunohistochemical studies have shown the presence of both the SNAT1 and SNAT2 SA protein in cortical astrocytes *in vivo* (Gonzalez-Gonzalez et al. 2005; Melone et al. 2004; Melone et al. 2006). The variability in reported astrocytic SA recordings could be due to the well documented regulation of SNAT2 by intracellular signalling mechanisms (Broer 2014). The magnitude of the SA-mediated current we observe (-20 pA) is almost identical to the magnitude of the SA current we record in the adjacent MNTB principal neurons (-21 pA, Blot et al. 2009), suggesting that *in situ* the glial expression of SA in this brain region is of a similar level to the neuronal expression. However, the majority of astrocytic SA is found in endfeet adjacent to endothelial basal lamina (Gonzalez-Gonzalez et al. 2005; Melone et al. 2004; Melone et al. 2006), which is in contrast to the perisynaptic location of SNAT3 (Boulland et al. 2002). This suggests a role for astrocytic SA in the import of glutamine into the brain across the blood brain barrier, rather than neurotransmitter recycling.

When the SA activity was inhibited with Li^+ or occluded with MeAIB, a very small glutamine induced current was still consistently observed. This could be due to uncoupled ion movements associated with activation of SN that have been observed following SN expression in oocytes (Broer et al. 2002; Chaudhry et al. 2001). However, the small magnitude of this current (< -2 pA) and large membrane conductance of astrocytes (Verkhratsky and Steinhauser 2000) suggests that this will not influence the membrane potential of astrocytes *in situ* and is therefore likely to be of little physiological consequence. The lack of significant SN mediated membrane current further supports the finding that SN

18

transport is electroneutral (Broer et al. 2002) and under physiological conditions it does not operate with the electrogenic stoichiometry suggested by Fei et al. (2000).

The electroneutrality of SN helps impart reversibility on the glutamine transport mechanism under physiological conditions and endows the potential for SN-mediated glutamine release. This has been shown in SNAT3 expressing *Xenopus* oocytes, where influx or efflux of radiolabelled glutamine can be observed by manipulation of the transmembrane pH gradient (Broer et al. 2002). Glutamine efflux from astrocytes can also be stimulated by EAAT activation, both in tissue culture (Broer et al. 2004) and in brain slices (Uwechue et al. 2012), although the mechanism triggering the release remained elusive. Using local neurons to monitor extracellular glutamine levels we have shown that this astrocytic glutamine release shows tight temporal coupling to activation of EAATs, and proposed that the trigger for glutamine release is the rise in $[Na^+]_i$ associated with EAAT activation (Uwechue et al. 2012). EAAT-mediated glutamate uptake is accompanied by the co-transport of three Na^+ (Zerangue and Kavanaugh 1996), which gives the potential for a significant $[Na^+]_i$ rise that would influence the thermodynamic equilibrium of SN and cause an efflux of glutamine. This is similar to the Na^+-facilitated mechanism proposed for the EAAT-induced release of GABA from astrocytes (Heja et al. 2009; Heja et al. 2012; Kirischuk et al. 2016).

To investigate the validity of this hypothesis, in this study we have demonstrated that in addition to SN transport being stimulated by a rise in glutamine concentration (in the continued presence of a transportable cation), SN transport can also be stimulated by a rise in cation concentration in the presence of glutamine. For these experiments we used Li^+ as the transported cation to isolate an SN-mediated cation-induced glutamine-dependent response, and increased the concentration from a baseline level of 20 mM to be consistent with the baseline level of $[Na^+]_i$ observed in astrocytes (Rose and Ransom 1996; Unichenko et al. 2012). Despite the affinity for Li^+ being ~30% of that for Na^+ (Kilberg et al. 1980), our results clearly show that alterations in cation concentration can drive SN transport is astrocytes *in situ*.

To further demonstrate that changes in $[Na^+]_i$ have the potential to directly influence SN, we used three separate approaches to raise astrocytic $[Na^+]_i$ and investigate the effect on glutamine transport. Activation of EAATs (with D-aspartate), SA (with MeAIB) and ionotropic glutamate receptors (with kainate) all significantly increased $[Na^+]_i$ and inhibited stimulated

glutamine influx, indicating that the thermodynamic equilibrium of SN has been altered by the change in $[Na^+]_i$. Although activation of EAATs caused a four-fold smaller $[Na^+]_i$ rise than activation of glutamate receptors, the effect on SN was more pronounced. This preferential influence on EAAT on SN may be a result of close physical coupling between SNAT3 and EAATs, analogous to that observed in Bergmann glia (Martinez-Lozada et al. 2013), which could create a local microdomain of Na^+ (Kirischuk et al. 2012; Rose and Karus 2013) and more heavily influence SN than AMPA receptors, which are expressed throughout the astrocyte but most strongly on the soma (Conti et al. 1994; Martin et al. 1993). Since brief periods of neuronal activity have been shown to increase astrocytic $[Na^+]_i$ by 10 – 15 mM (Bennay et al. 2008; Kirischuk et al. 2007; Langer and Rose 2009), $[Na^+]_i$ has the potential to dynamically link neuronal activity to neurotransmitter supply. Our results therefore highlight the significance of the spatio-temporal regulation of $[Na^+]_i$ in astrocytes and the importance of Na^+ dynamics in regulating astrocytic function (Rose and Verkhratsky 2016).

Using a flux model of SNAT3 transport we have investigated the ability of EAAT activation to cause glutamine efflux by reversal of SNAT3. The model shows that the intracellular changes resulting from EAAT activation cause the efflux of glutamine, and that the rise in $[Na^+]_i$ is the main driving force for glutamine release. The model only considers fluxes at the cell soma, whereas in reality the glutamate influx and glutamine release occur in astrocyte processes (Boulland et al. 2002; Danbolt 2001). Local microdomains of Na^+ and H^+ changes are likely to be generated which would have a more profound effect on glutamine release. EAAT induced acidification opposes glutamine efflux, however, such pH changes are more rapidly buffered than the change in $[Na^+]_i$, which persist for 10s of seconds (Bennay et al. 2008; Kirischuk et al. 2007; Langer and Rose 2009). Although bicarbonate was omitted from our experimental solutions, the added pH buffering power that it endows will reduce the EAAT-mediated acidification and thus enhance glutamine release. The model assumes that the apparent affinity of the transporter for the substrates is constant and unaffected by changes in substrate concentration. This is known not to be true. For example, changes in extracellular pH alter the apparent affinity of SNAT3 for Na^+ (Broer et al. 2002; Chaudhry et al. 2001). However, the relatively small changes in ion concentrations that we observe are unlikely to have a significant influence on the output of the model and our conclusions would remain valid.

Our data presented here show that SNAT3 is functionally expressed in perisynaptic astrocytes *in situ* and establish a clear functional link between EAAT activation and

20

glutamine transport via changes in $[Na^+]_i$. This strongly supports a role for astrocytes at synapses that involves detecting locally released glutamate and releasing glutamine in a tightly regulated manner (Uwechue et al. 2012), which in turn could be sequestered by presynaptic terminals to replace neurotransmitter as part of a glutamate-glutamine cycle.

Acknowledgements

22

References

Baird FE, Beattie KJ, Hyde AR, Ganapathy V, Rennie MJ, Taylor PM. 2004. Bidirectional substrate fluxes through the system N (SNAT5) glutamine transporter may determine net glutamine flux in rat liver. J Physiol 559(Pt 2):367-81.

Bak LK, Schousboe A, Waagepetersen HS. 2006. The glutamate/GABA-glutamine cycle: aspects of transport, neurotransmitter homeostasis and ammonia transfer. J Neurochem 98(3):641-53.

Bennay M, Langer J, Meier SD, Kafitz KW, Rose CR. 2008. Sodium signals in cerebellar Purkinje neurons and Bergmann glial cells evoked by glutamatergic synaptic transmission. Glia 56(10):1138-49.

Billups D, Marx MC, Mela I, Billups B. 2013. Inducible presynaptic glutamine transport supports glutamatergic transmission at the calyx of Held synapse. J Neurosci 33(44):17429-34.

Blot A, Billups D, Bjorkmo M, Quazi AZ, Uwechue NM, Chaudhry FA, Billups B. 2009. Functional expression of two system A glutamine transporter isoforms in rat auditory brainstem neurons. Neuroscience 164(3):998-1008.

Boulland JL, Osen KK, Levy LM, Danbolt NC, Edwards RH, Storm-Mathisen J, Chaudhry FA. 2002. Cell-specific expression of the glutamine transporter SN1 suggests differences in dependence on the glutamine cycle. Eur J Neurosci 15(10):1615-31.

Boulland JL, Rafiki A, Levy LM, Storm-Mathisen J, Chaudhry FA. 2003. Highly differential expression of SN1, a bidirectional glutamine transporter, in astroglia and endothelium in the developing rat brain. Glia 41(3):260-75.

Broer A, Albers A, Setiawan I, Edwards RH, Chaudhry FA, Lang F, Wagner CA, Broer S. 2002. Regulation of the glutamine transporter SN1 by extracellular pH and intracellular sodium ions. J Physiol 539(Pt 1):3-14.

Broer A, Brookes N, Ganapathy V, Dimmer KS, Wagner CA, Lang F, Broer S. 1999. The astroglial ASCT2 amino acid transporter as a mediator of glutamine efflux. J Neurochem 73(5):2184-94.

Broer A, Deitmer JW, Broer S. 2004. Astroglial glutamine transport by system N is upregulated by glutamate. Glia 48(4):298-310.

Broer A, Wagner CA, Lang F, Broer S. 2000. The heterodimeric amino acid transporter 4F2hc/y+LAT2 mediates arginine efflux in exchange with glutamine. Biochem J 349 Pt 3:787-95.

Broer S. 2014. The SLC38 family of sodium-amino acid co-transporters. Pflugers Arch 466(1):155-72.

Chaudhry FA, Krizaj D, Larsson P, Reimer RJ, Wreden C, Storm-Mathisen J, Copenhagen D, Kavanaugh M, Edwards RH. 2001. Coupled and uncoupled proton movement by amino acid transport system N. EMBO J 20(24):7041-51.

Chaudhry FA, Reimer RJ, Krizaj D, Barber D, Storm-Mathisen J, Copenhagen DR, Edwards RH. 1999. Molecular analysis of system N suggests novel physiological roles in nitrogen metabolism and synaptic transmission. Cell 99(7):769-80.

Chaudhry FA, Schmitz D, Reimer RJ, Larsson P, Gray AT, Nicoll R, Kavanaugh M, Edwards RH. 2002. Glutamine uptake by neurons: interaction of protons with system a transporters. J Neurosci 22(1):62-72.

Conti F, Minelli A, Brecha NC. 1994. Cellular localization and laminar distribution of AMPA glutamate receptor subunits mRNAs and proteins in the rat cerebral cortex. J Comp Neurol 350(2):241-59.

Cubelos B, Gonzalez-Gonzalez IM, Gimenez C, Zafra F. 2005. Amino acid transporter SNAT5 localizes to glial cells in the rat brain. Glia 49(2):230-44.

Daikhin Y, Yudkoff M. 2000. Compartmentation of brain glutamate metabolism in neurons and glia. J Nutr 130(4S Suppl):1026S-31S.

Danbolt NC. 2001. Glutamate uptake. Prog Neurobiol 65(1):1-105.

Deitmer JW, Broer A, Broer S. 2003. Glutamine efflux from astrocytes is mediated by multiple pathways. J Neurochem 87(1):127-35.

Dolinska M, Zablocka B, Sonnewald U, Albrecht J. 2004. Glutamine uptake and expression of mRNA's of glutamine transporting proteins in mouse cerebellar and cerebral cortical astrocytes and neurons. Neurochem Int 44(2):75-81.

Fei YJ, Sugawara M, Nakanishi T, Huang W, Wang H, Prasad PD, Leibach FH, Ganapathy V. 2000. Primary structure, genomic organization, and functional and electrogenic characteristics of human system N 1, a Na+- and H+-coupled glutamine transporter. J Biol Chem 275(31):23707-17.

Fricke MN, Jones-Davis DM, Mathews GC. 2007. Glutamine uptake by System A transporters maintains neurotransmitter GABA synthesis and inhibitory synaptic transmission. J Neurochem 102(6):1895-904.

Gonzalez-Gonzalez IM, Cubelos B, Gimenez C, Zafra F. 2005. Immunohistochemical localization of the amino acid transporter SNAT2 in the rat brain. Neuroscience 130(1):61-73.

Gu S, Roderick HL, Camacho P, Jiang JX. 2000. Identification and characterization of an amino acid transporter expressed differentially in liver. Proc Natl Acad Sci U S A 97(7):3230-5.

Hagglund MG, Sreedharan S, Nilsson VC, Shaik JH, Almkvist IM, Backlin S, Wrange O, Fredriksson R. 2011. Identification of SLC38A7 (SNAT7) protein as a glutamine transporter expressed in neurons. J Biol Chem 286(23):20500-11.

Hamdani el H, Gudbrandsen M, Bjorkmo M, Chaudhry FA. 2012. The system N transporter SN2 doubles as a transmitter precursor furnisher and a potential regulator of NMDA receptors. Glia 60(11):1671-83.

Heckel T, Broer A, Wiesinger H, Lang F, Broer S. 2003. Asymmetry of glutamine transporters in cultured neural cells. Neurochem Int 43(4-5):289-98.

Heja L, Barabas P, Nyitrai G, Kekesi KA, Lasztoczi B, Toke O, Tarkanyi G, Madsen K, Schousboe A, Dobolyi A and others. 2009. Glutamate uptake triggers transporter-mediated GABA release from astrocytes. PLoS One 4(9):e7153.

Heja L, Nyitrai G, Kekesi O, Dobolyi A, Szabo P, Fiath R, Ulbert I, Pal-Szenthe B, Palkovits M, Kardos J. 2012. Astrocytes convert network excitation to tonic inhibition of neurons. BMC Biol 10:26.

Hertz L, Dringen R, Schousboe A, Robinson SR. 1999. Astrocytes: glutamate producers for neurons. J Neurosci Res 57(4):417-28.

Jacobson I, Sandberg M, Hamberger A. 1985. Mass transfer in brain dialysis devices--a new method for the estimation of extracellular amino acids concentration. J Neurosci Methods 15(3):263-8.

Jiang E, Yan X, Weng HR. 2012. Glial glutamate transporter and glutamine synthetase regulate GABAergic synaptic strength in the spinal dorsal horn. J Neurochem.

Kanamori K, Ross BD. 2004. Quantitative determination of extracellular glutamine concentration in rat brain, and its elevation in vivo by system A transport inhibitor, alpha-(methylamino)isobutyrate. J Neurochem 90(1):203-10.

Kilberg MS, Handlogten ME, Christensen HN. 1980. Characteristics of an amino acid transport system in rat liver for glutamine, asparagine, histidine, and closely related analogs. J Biol Chem 255(9):4011-9.

Kimelberg HK, Schools GP, Cai Z, Zhou M. 2000. Freshly isolated astrocyte (FIA) preparations: a useful single cell system for studying astrocyte properties. J Neurosci Res 61(6):577-87.

Kirischuk S, Heja L, Kardos J, Billups B. 2016. Astrocyte sodium signaling and the regulation of neurotransmission. Glia 64(10):1655-66.

Kirischuk S, Kettenmann H, Verkhratsky A. 2007. Membrane currents and cytoplasmic sodium transients generated by glutamate transport in Bergmann glial cells. Pflugers Arch 454(2):245-52.

Kirischuk S, Parpura V, Verkhratsky A. 2012. Sodium dynamics: another key to astroglial excitability? Trends Neurosci 35(8):497-506.

Laake JH, Slyngstad TA, Haug FM, Ottersen OP. 1995. Glutamine from glial cells is essential for the maintenance of the nerve terminal pool of glutamate: immunogold evidence from hippocampal slice cultures. J Neurochem 65(2):871-81.

Langer J, Rose CR. 2009. Synaptically induced sodium signals in hippocampal astrocytes in situ. J Physiol 587(Pt 24):5859-77.

Liang SL, Carlson GC, Coulter DA. 2006. Dynamic regulation of synaptic GABA release by the glutamate-glutamine cycle in hippocampal area CA1. J Neurosci 26(33):8537-48.

Mackenzie B, Schafer MK, Erickson JD, Hediger MA, Weihe E, Varoqui H. 2003. Functional properties and cellular distribution of the system A glutamine transporter SNAT1 support specialized roles in central neurons. J Biol Chem 278(26):23720-30.

Martin LJ, Blackstone CD, Levey AI, Huganir RL, Price DL. 1993. AMPA glutamate receptor subunits are differentially distributed in rat brain. Neuroscience 53(2):327-58.

Martinez-Lozada Z, Guillem AM, Flores-Mendez M, Hernandez-Kelly LC, Vela C, Meza E, Zepeda RC, Caba M, Rodriguez A, Ortega A. 2013. GLAST/EAAT1-induced glutamine release via SNAT3 in Bergmann glial cells: evidence of a functional and physical coupling. J Neurochem 125(4):545-54.

Marx MC, Billups D, Billups B. 2015. Maintaining the presynaptic glutamate supply for excitatory neurotransmission. J Neurosci Res 93(7):1031-44.

McKenna MC. 2007. The glutamate-glutamine cycle is not stoichiometric: fates of glutamate in brain. J Neurosci Res 85(15):3347-58.

Melone M, Quagliano F, Barbaresi P, Varoqui H, Erickson JD, Conti F. 2004. Localization of the glutamine transporter SNAT1 in rat cerebral cortex and neighboring structures, with a note on its localization in human cortex. Cereb Cortex 14(5):562-74.

Melone M, Varoqui H, Erickson JD, Conti F. 2006. Localization of the Na(+)-coupled neutral amino acid transporter 2 in the cerebral cortex. Neuroscience 140(1):281-92.

Minta A, Tsien RY. 1989. Fluorescent indicators for cytosolic sodium. J Biol Chem 264(32):19449-57.

Muller J, Reyes-Haro D, Pivneva T, Nolte C, Schaette R, Lubke J, Kettenmann H. 2009. The principal neurons of the medial nucleus of the trapezoid body and NG2(+) glial cells receive coordinated excitatory synaptic input. J Gen Physiol 134(2):115-27.

Nagaraja TN, Brookes N. 1996. Glutamine transport in mouse cerebral astrocytes. J Neurochem 66(4):1665-74.

Nakanishi T, Kekuda R, Fei YJ, Hatanaka T, Sugawara M, Martindale RG, Leibach FH, Prasad PD, Ganapathy V. 2001a. Cloning and functional characterization of a new subtype of the amino acid transport system N. Am J Physiol Cell Physiol 281(6):C1757-68.

Nakanishi T, Sugawara M, Huang W, Martindale RG, Leibach FH, Ganapathy ME, Prasad PD, Ganapathy V. 2001b. Structure, function, and tissue expression pattern of human SN2, a subtype of the amino acid transport system N. Biochem Biophys Res Commun 281(5):1343-8.

Norenberg MD, Martinez-Hernandez A. 1979. Fine structural localization of glutamine synthetase in astrocytes of rat brain. Brain Res 161(2):303-10.

Ottersen OP, Zhang N, Walberg F. 1992. Metabolic compartmentation of glutamate and glutamine: morphological evidence obtained by quantitative immunocytochemistry in rat cerebellum. Neuroscience 46(3):519-34.

Patel AJ, Hunt A. 1985. Concentration of free amino acids in primary cultures of neurones and astrocytes. J Neurochem 44(6):1816-21.

Patneau DK, Mayer ML. 1990. Structure-activity relationships for amino acid transmitter candidates acting at N-methyl-D-aspartate and quisqualate receptors. J Neurosci 10(7):2385-99.

Perea G, Navarrete M, Araque A. 2009. Tripartite synapses: astrocytes process and control synaptic information. Trends Neurosci 32(8):421-31.

Pineda M, Fernandez E, Torrents D, Estevez R, Lopez C, Camps M, Lloberas J, Zorzano A, Palacin M. 1999. Identification of a membrane protein, LAT-2, that Co-expresses with 4F2 heavy chain,

an L-type amino acid transport activity with broad specificity for small and large zwitterionic amino acids. J Biol Chem 274(28):19738-44.

Rae C, Hare N, Bubb WA, McEwan SR, Broer A, McQuillan JA, Balcar VJ, Conigrave AD, Broer S. 2003. Inhibition of glutamine transport depletes glutamate and GABA neurotransmitter pools: further evidence for metabolic compartmentation. J Neurochem 85(2):503-14.

Rajan DP, Kekuda R, Huang W, Devoe LD, Leibach FH, Prasad PD, Ganapathy V. 2000. Cloning and functional characterization of a Na(+)-independent, broad-specific neutral amino acid transporter from mammalian intestine. Biochim Biophys Acta 1463(1):6-14.

Reichel A, Begley DJ, Ermisch A. 1995. Changes in amino acid levels in rat plasma, cisternal cerebrospinal fluid, and brain tissue induced by intravenously infused arginine-vasopressin. Peptides 16(5):965-71.

Reyes-Haro D, Muller J, Boresch M, Pivneva T, Benedetti B, Scheller A, Nolte C, Kettenmann H. 2010. Neuron-astrocyte interactions in the medial nucleus of the trapezoid body. J Gen Physiol 135(6):583-94.

Rodriguez A, Ortega A, Berumen LC, Garcia-Alcocer MG, Gimenez C, Zafra F. 2014. Expression of the System N transporter (SNAT5/SN2) during development indicates its plausible role in glutamatergic neurotransmission. Neurochem Int 73:166-71.

Rose CR, Karus C. 2013. Two sides of the same coin: sodium homeostasis and signaling in astrocytes under physiological and pathophysiological conditions. Glia 61(8):1191-205.

Rose CR, Ransom BR. 1996. Intracellular sodium homeostasis in rat hippocampal astrocytes. J Physiol 491 (Pt 2):291-305.

Rose CR, Verkhratsky A. 2016. Principles of sodium homeostasis and sodium signalling in astroglia. Glia 64(10):1611-27.

Rothman DL, Behar KL, Hyder F, Shulman RG. 2003. In vivo NMR studies of the glutamate neurotransmitter flux and neuroenergetics: implications for brain function. Annu Rev Physiol 65:401-27.

Rowland KC, Irby NK, Spirou GA. 2000. Specialized synapse-associated structures within the calyx of Held. J Neurosci 20(24):9135-44.

Sands SB, Barish ME. 1989. NMDA receptor activation by residual glutamate in glutamine preparations: a cautionary note regarding weak NMDA receptor agonists. Brain Res 495(1):193-7.

Satzler K, Sohl LF, Bollmann JH, Borst JG, Frotscher M, Sakmann B, Lubke JH. 2002. Three-dimensional reconstruction of a calyx of Held and its postsynaptic principal neuron in the medial nucleus of the trapezoid body. J Neurosci 22(24):10567-79.

Schneggenburger R, Forsythe ID. 2006. The calyx of Held. Cell Tissue Res 326(2):311-37.

Schousboe A, Hertz L, Svenneby G, Kvamme E. 1979. Phosphate activated glutaminase activity and glutamine uptake in primary cultures of astrocytes. J Neurochem 32(3):943-50.

Segawa H, Fukasawa Y, Miyamoto K, Takeda E, Endou H, Kanai Y. 1999. Identification and functional characterization of a Na+-independent neutral amino acid transporter with broad substrate selectivity. J Biol Chem 274(28):19745-51.

Sidoryk-Wegrzynowicz M, Lee E, Albrecht J, Aschner M. 2009. Manganese disrupts astrocyte glutamine transporter expression and function. J Neurochem 110(3):822-30.

Sidoryk M, Obara M, Albrecht J. 2006. Selective decrease of SN1(SNAT3) mRNA expression in human and rat glioma cells adapted to grow in acidic medium. Neurochem Int 48(6-7):547-52.

Smith PH, Joris PX, Yin TC. 1998. Anatomy and physiology of principal cells of the medial nucleus of the trapezoid body (MNTB) of the cat. J Neurophysiol 79(6):3127-42.

Sonnewald U, Westergaard N, Schousboe A, Svendsen JS, Unsgard G, Petersen SB. 1993. Direct demonstration by [13C]NMR spectroscopy that glutamine from astrocytes is a precursor for GABA synthesis in neurons. Neurochem Int 22(1):19-29.

Tani H, Dulla CG, Farzampour Z, Taylor-Weiner A, Huguenard JR, Reimer RJ. 2014. A local glutamate-glutamine cycle sustains synaptic excitatory transmitter release. Neuron 81(4):888-900.

Tani H, Dulla CG, Huguenard JR, Reimer RJ. 2010. Glutamine is required for persistent epileptiform activity in the disinhibited neocortical brain slice. J Neurosci 30(4):1288-300.

Taylor PM, Mackenzie B, Low SY, Rennie MJ. 1992. Expression of rat liver glutamine transporters in Xenopus laevis oocytes. J Biol Chem 267(6):3873-7.

Theparambil SM, Deitmer JW. 2015. High effective cytosolic H+ buffering in mouse cortical astrocytes attributable to fast bicarbonate transport. Glia 63(9):1581-94.

Theparambil SM, Naoshin Z, Thyssen A, Deitmer JW. 2015. Reversed electrogenic sodium bicarbonate cotransporter 1 is the major acid loader during recovery from cytosolic alkalosis in mouse cortical astrocytes. J Physiol 593(16):3533-47.

Unichenko P, Myakhar O, Kirischuk S. 2012. Intracellular Na+ concentration influences short-term plasticity of glutamate transporter-mediated currents in neocortical astrocytes. Glia 60(4):605-14.

Utsunomiya-Tate N, Endou H, Kanai Y. 1996. Cloning and functional characterization of a system ASC-like Na+-dependent neutral amino acid transporter. J Biol Chem 271(25):14883-90.

Uwechue NM, Marx MC, Chevy Q, Billups B. 2012. Activation of glutamate transport evokes rapid glutamine release from perisynaptic astrocytes. J Physiol 590(Pt 10):2317-2331.

Verkhratsky A, Steinhauser C. 2000. Ion channels in glial cells. Brain Res Brain Res Rev 32(2-3):380-412.

Willoughby D, Thomas RC, Schwiening CJ. 1998. Comparison of simultaneous pH measurements made with 8-hydroxypyrene-1,3,6-trisulphonic acid (HPTS) and pH-sensitive microelectrodes in snail neurones. Pflugers Arch 436(4):615-22.

Yamada KA, Rothman SM. 1989. Glutamine currents in hippocampal neurons are attributable to contaminating glutamate. Brain Res 498(2):351-4.

Yang S, Cox CL. 2011. Attenuation of inhibitory synaptic transmission by glial dysfunction in rat thalamus. Synapse 65(12):1298-308.

Zerangue N, Kavanaugh MP. 1996. Flux coupling in a neuronal glutamate transporter. Nature 383(6601):634-7.

Zielinska M, Dabrowska K, Hadera MG, Sonnewald U, Albrecht J. 2016. System N transporters are critical for glutamine release and modulate metabolic fluxes of glucose and acetate in cultured cortical astrocytes: changes induced by ammonia. J Neurochem 136(2):329-38.

Figure Legends

FIGURE 1: Voltage-clamped astrocytes exhibit a glutamine-induced current. **(A)** DIC image of a brainstem slice. An astrocyte (*) located adjacent to a principal cell of the MNTB (#) was whole-cell patch-clamped by an electrode (‡). Two puffer pipettes (†) were positioned near to the astrocyte. Scale bar = 25 µm. **(B)** Example current-voltage relationship of a voltage-clamped astrocyte, showing a characteristically linear relationship with a hyperpolarized membrane potential (mean of -80.8 ± 0.2 mV) and low membrane resistance (2.9 ± 0.3 MΩ; n = 167). **(C)** Example astrocytic current elicited by a 5 s puff of 10 mM glutamine in standard aCSF (black trace) and Na^+-free Li^+-aCSF (grey trace). **(D)** The relative astrocytic current was significantly reduced when glutamine was puffed in the presence of Li^+-aCSF (n = 6) or 20 mM MeAIB (n = 4) compared to control aCSF (** P < 0.01).

FIGURE 2: Glutamine applications causes $[Na^+]_i$ and pH_i changes in astrocytes. **(A)** Change of somatic pH over time, recorded with HPTS in the patch-pipette with applications of increasing bath glutamine concentrations of 0, 0.5, 2 and 20 mM. **(B)** Dose-response curve showing the average change in astrocytic pH_i relative to 20 mM for 0.5, 1, 2, 5, 10 & 20 mM glutamine solutions (n = 4 for 0.5, 1 & 2 mM; n = 3 for 5 & 10 mM; n = 8 for 20 mM). The data were well-fit with a Michaelis-Menten relationship (K_M = 1.57 mM; black line, least-squares fit). **(C-D)** 10 mM glutamine puff application (black bar) caused an astrocytic alkalinisation. This alkalisation was not seen for puffs of aCSF (grey bar; response was significantly smaller than control; *** P < 0.001). **(E-F)** Astrocytic alkalinisation in response to 10 mM glutamine puffs (black bar) remained unchanged when the EAAT inhibitor TFB-TBOA (grey line; 20 µM) was added to the aCSF (the mean response relative to control = 1.03 ± 0.04; n = 5; P = 0.75). The response to glutamine puffs also remained when a mixture of channel inhibitors was included in the aCSF (APV, MK-801, NBQX, TTX, strychnine and bicuculline), with a slightly larger response to glutamine puffs observed (the mean relative response = 1.19 ± 0.13; n = 4; * P = 0.02). **(G-H)** Astrocytic somatic $[Na^+]_i$, measured with SBFI in the patch-pipette, increased in response to puff application of 10 mM glutamine (black bar). This response was not inhibited by the inclusion of 20 µM TFB-TBOA in the aCSF (grey trace; n = 4; P = 0.7).

FIGURE 3: Astrocytic glutamine transport is Na^+ dependent and Li^+ tolerant. **(A)** Puff application of 10 mM glutamine (black bar) elicited an astrocytic alkalinisation (black line),

which was eliminated when external Na^+ was replaced by NMDG (grey line). This inhibition was reversed when Na^+ was reintroduced (dotted line). **(B)** The astrocytic pH_i response to 10 mM glutamine puffs (black line) remained unchanged when Na^+ was replaced with Li^+ in the external solution (grey line). **(C)** The astrocytic pH_i response to glutamine puffs (black line) was occluded by bath application of 20 mM histidine (grey line). **(D)** The astrocytic pH_i response to glutamine puffs was maintained over time following Li^+ substitution for Na^+ (black line). Conversely, when Na^+ was replaced by NMDG the response to glutamine puffs decayed as Na^+ was washed out of the bath. **(E)** Averaged data showing no change in astrocytic pH_i response to 10 mM glutamine when Na^+ was substituted with Li^+. However replacement of Na^+ with NMDG significantly reduced the response to glutamine. Addition of 20 mM Histidine to the aCSF significantly blocked the response to glutamine puffs, whereas addition of 20 mM leucine had no effect on the astrocytic response to glutamine (*** $P < 0.0001$).

FIGURE 4: Substrate profile of the astrocytic glutamine transporter is consistent with SNAT3. **(A-F)** Astrocytic alkalinisation in response to puff application of 10 mM glutamine (black trace) compared to application of another amino acid (10 mM) from a second adjacent puff-pipette (grey traces; single amino acid codes; m = MeAIB), for histidine **(A)**, asparagine **(B)**, alanine **(C)**, serine **(D)**, leucine **(E)** and MeAIB **(F)**. **(G)** Averaged data showing a significant astrocytic alkalinisation in response to glutamine (Q), histidine (H) or asparagine (N), a small but statistically insignificant effect of alanine (A), and no response to serine (S), leucine (L) or MeAIB application. (* $P = 0.05$; ** $P < 0.01$; *** $P < 0.001$). Alanine and serine where both applied in the presence of TFB-TBOA (20 μM) to prevent activation of EAAT-family transporters.

FIGURE 5: Increase in cation concentration can induce SNAT3 activity. **(A)** Puff application of 150 mM Li^+ (black bar) in a 20 mM Li^+ aCSF background external solution caused no change in astrocytic pH_i when no glutamine was present (-Q; grey trace). However, when 20 mM glutamine was included in the external solution, puff application of 150 mM Li^+ induced an astrocytic alkalinisation (+Q, black trace). **(B)** The pH_i response to puffs of high concentration Li^+ are significantly greater when 20 mM glutamine (+Q) is present in the aCSF (n = 4; * $P < 0.05$).

FIGURE 6: Glutamate receptor and transporter activation increases astrocytic sodium concentration. **(A)** Application of the EAAT substrate D-aspartate (200 µM; black bar) induced an inward current in astrocytes voltage-clamped at -80 mV (black trace), which was completely inhibited by TFB-TBOA (20 µM; grey trace). **(B)** D-aspartate application (200 µM; black bar) was accompanied by an increase in astrocytic $[Na^+]_i$ (black trace), which was likewise inhibited by the addition of TFB-TBOA (20 µM; grey trace). **(C)** Averaged data showing that the astrocytic EAAT current was inhibited by TFB-TBOA (n = 4; ** $P < 0.01$). Similarly, the EAAT-mediated increase in astrocytic $[Na^+]_i$ was also inhibited by TFB-TBOA (n = 4; * $P < 0.05$). **(D)** EAAT activation by bath application of D-aspartate (200 µM; black bar) caused a sustained increase of astrocytic $[Na^+]_i$ (average data from 3 cells). **(E)** Addition of the system A substrate MeAIB (20 mM; black bar) to the bath lead to an increase in astrocytic $[Na^+]_i$ (average data from 4 cells). **(F)** AMPAR activation by bath application of kainate (300 µM; black bar) caused an increase in astrocytic $[Na^+]_i$ (average data from 3 cells). Kainate experiments were performed in the presence of TTX, bicuculline, AP5 and MK801 to limit any potential neuronal activity.

FIGURE 7: Increasing astrocytic $[Na^+]_i$ by EAAT activation reduces SNAT3 mediated glutamine influx. **(A)** Puff application of 10 mM glutamine (black bar) elicited an astrocytic alkalinisation (black line), which was reduced when 200 µM D-aspartate was bath applied (dark grey). Addition of TFB-TBOA (20 µM) to the bath rescued the glutamine-induced response (light grey). **(B)** Averaged data showing the reduction in glutamine-induced alkalinisation by D-aspartate (58 ± 6 % of control; n = 4; *** $P < 0.001$) and its rescue by presence of TFB-TBOA (106 ± 4 % of control response, n = 3; $P = 0.70$). **(C)** Using a physiological $[Na^+]_i$ of 15 mM, bath application of 200 µM D-aspartate (grey trace) similarly reduced the glutamine elicited alkalinisation compared to control (black trace). **(D)** Averaged data showing the reduction in glutamine-induced alkalinisation by D-aspartate with 15 mM Na^+_i (67 ± 8 % of control; n = 4; *** $P < 0.001$). **(E)** Averaged data from 4 cells showing the time-dependence of the D-aspartate effect in panels B and C. Glutamine puffs induced an astrocytic alkalinisation that was inhibited by bath application of 200 µM D-aspartate (black bar).

FIGURE 8: Increasing astrocytic $[Na^+]_i$ by SA and AMPA receptor activation reduces SNAT3 mediated glutamine influx. **(A)** Bath application of MeAIB (20 mM; grey trace) reduced the astrocytic pH_i response to glutamine puffs. **(B)** Averaged data showing the reduction in glutamine-induced alkalinisation by MeAIB (68 ± 5 % of control response; n = 10; *** $P <$

30

0.001). **(C)** Bath application of kainate (300 μM; dark grey trace) reduced the astrocytic pH_i response to glutamine puffs. Addition of NBQX (20 μM) to the bath prevented the kainate-induced decrease in glutamine response (light grey). **(D)** Averaged data showing the reduction in glutamine-induced alkalinisation by kainate (75 ± 5 % of control; n = 4; ** P < 0.01) and its rescue by presence of NBQX (106 ± 4 % of control response; n = 3; P = 0.55). **(E)** Averaged data showing the time-dependence of the kainate effect in panels C and D. Glutamine puffs induced an astrocytic alkalinisation that was inhibited by bath application of 300 μM kainate (black points) over a period of 5 minutes. Inclusion of 20 μM NBQX in the perfusing medium inhibited the effect of kainate (grey points).

FIGURE 9: Model of SNAT3 mediated fluxes shows glutamine release upon EAAT activation. **(A)** SNAT3 activation by external application of glutamine (5 s, 0.89 mM puff; black bar) causes a positive flux (glutamine influx), internal alkalinisation, rise of $[Na^+]_i$ and increase in $[Gln]_i$. **(B)** Activation of EAATs by external application of D-aspartate (which is not metabolised to internal glutamine) causes a negative flux (release of glutamine), internal acidification, rise of $[Na^+]_i$ and reduction of $[Gln]_i$. **(C)** Activation of EAATs by external application of glutamate (which is subsequently metabolised to glutamine; bottom panel) causes an increased efflux compared to D-aspartate, and similar acidification and rise of $[Na^+]_i$.

FIGURE 10: Glutamine efflux is driven mainly by changes in $[Na^+]_i$. **(A)** Model of SNAT3 mediated flux upon EAAT application (glutamate; black bar), stimulated by the EAAT-mediated $[Na^+]_i$ change only (EAAT-mediated pH_i and $[Gln]_i$ changes are ignored). **(B)** SNAT3 fluxes upon EAAT activation driven by the EAAT-mediated pH_i change only (EAAT-mediated $[Na^+]_i$ and $[Gln]_i$ changes are ignored). **(C)** SNAT3 fluxes upon EAAT activation driven by the EAAT-mediated $[Gln]_i$ change only (EAAT-mediated $[Na^+]_i$ and pH_i changes are ignored). Of the EAAT-mediated changes, $[Na^+]_i$ has the greatest influence on the SNAT3 flux (panel A).

FIGURE 11: SNAT3 mediated glutamine efflux is stimulated by $[Na^+]_i$ and forms part of the glutamate-glutamine cycle. Glutamate released from presynaptic terminals activates glutamate receptors, such as NMDA receptors (NMDAR) and AMPA receptors (AMPAR) on postsynaptic neurons. It is removed from the synaptic cleft by sequestration into neighbouring astrocytes via EAAT glutamate transporters, where it is converted into

31

glutamine by the astrocytic enzyme glutamine synthetase (GS). Astrocytic glutamate uptake initiates a rapid $[Na^+]_i$ signal in astrocytes, which influences the SNAT3 thermodynamic equilibrium to facilitate the efflux of glutamine. Extracellular glutamine is then transported into presynaptic terminals by an unidentified mechanism, and is subsequently converted to glutamate by the enzyme phosphate activated glutaminase (PAG) to resupply the presynaptic neurotransmitter pool.

SUPPLEMENTARY FIGURE 1. pH_i responses to puff-application of substrates in bicarbonate buffered external solution contain artefacts. Experiments in this figure were performed in external solution composed of (in mM) 145 NaCl, 2.5 KCl, 26 $NaHCO_3$, 1.25 NaH_2PO_4, 10 glucose, 1 $MgCl_2$, 2 $CaCl_2$; pH 7.3 set by saturating with 95/5% O_2/CO_2. A cocktail of compounds to inhibit ion channels was also included in external and puff solutions (40 µM APV, 10 µM MK-801, 20 µM NBQX, 1 µM TTX, 1 µM strychnine and 10 µM bicuculline). **(A)** Raw-data from two separate cells show that puff-application of 10 mM glutamine elicited an astrocytic alkalinisation. However, puff-application of external solution also produced a significant alkalinisation. **(B)** Averaged data showing the magnitude of the puff-artefact, which was 22 ± 10% (mean ± SEM; n = 7) of the glutamine-induced response (n = 8) and exhibited considerable variation. **(C)** Example data from one cell showing that puff-application of 10 mM glutamine (Q; black bar) elicited an astrocytic alkalinisation, which was subsequently reduced by the addition of 10 mM histidine to the external medium. **(D)** Averaged data showing that saturation of the SNAT3 response by histidine reduced the glutamine-induced alkalinisation by 77.0 ± 2.5 % (n = 3; P = 0.002; paired t-test). However, unlike in HEPES buffered solution (Fig. 3C, E), substrate inhibition of SNAT3 by histidine did not completely eliminate the response to glutamine due to the underlying puff-artefact.

32

A

B

4 nA

10 ms

I (nA)

8

4

Vm (mV)

-160 -120 -80 -40 0 40

-4

-8

C

Gln

Control

10 pA

5 s

Gln

In Li⁻

D

1.2

1

0.8

0.6

0.4

0.2

0

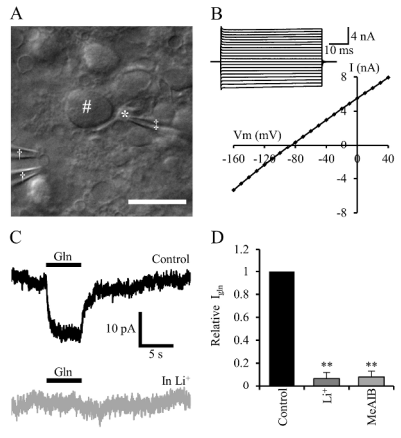Relative I_Gln

Control

Li⁺

MeAIB

**

**

FIGURE 1

FIGURE 1: Voltage-clamped astrocytes exhibit a glutamine-induced current.
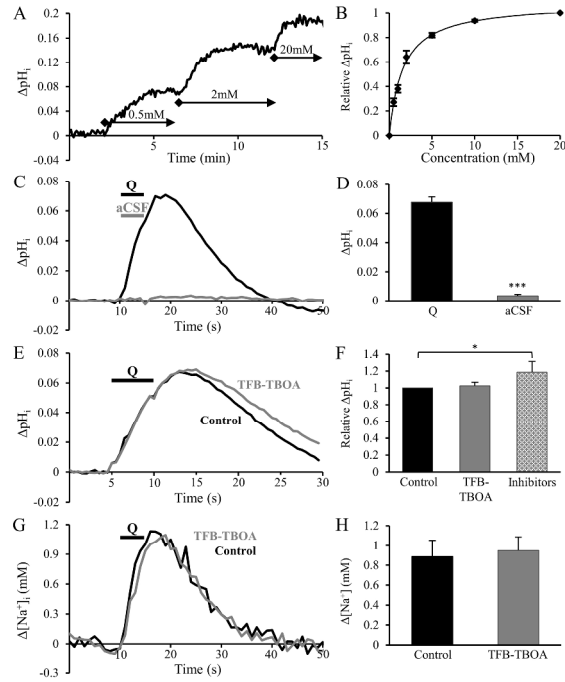Fig. 1
275x397mm (300 x 300 DPI)

FIGURE 2

FIGURE 2: Glutamine applications causes $[Na^+]_i$ and pH_i changes in astrocytes.
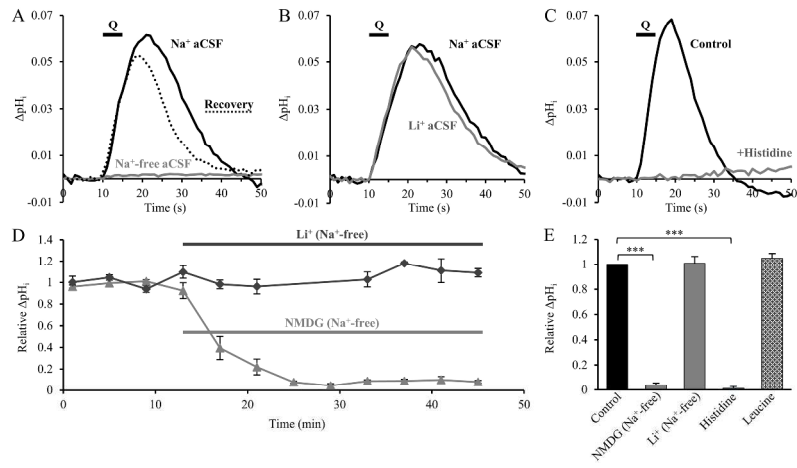Fig. 2
275x397mm (300 x 300 DPI)

FIGURE 3

FIGURE 3: Astrocytic glutamine transport is Na$^+$ dependent and Li$^+$ tolerant.
Fig. 3
275x397mm (300 x 300 DPI)
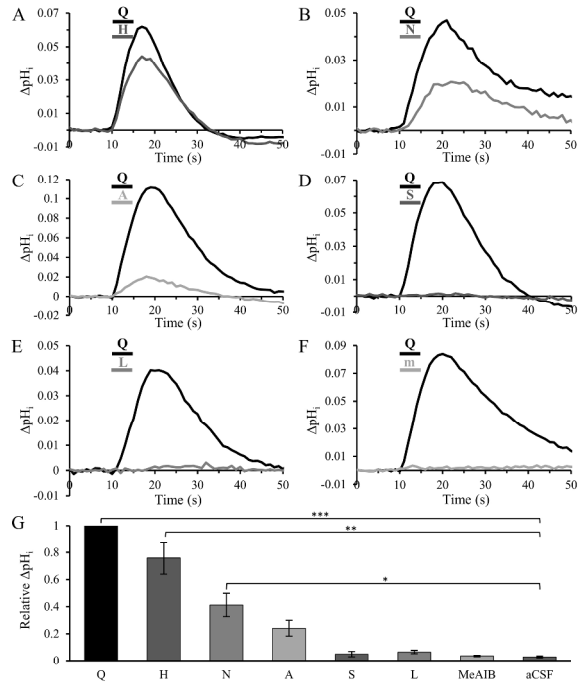
FIGURE 4

FIGURE 4: Substrate profile of the astrocytic glutamine transporter is consistent with SNAT3.
Fig. 4
275x397mm (300 x 300 DPI)

A

B
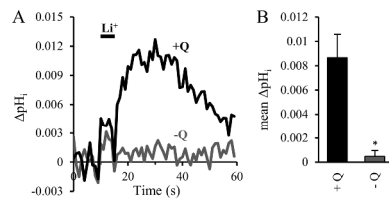
FIGURE 5

FIGURE 5: Increase in cation concentration can induce SNAT3 activity.
Fig. 5
275x397mm (300 x 300 DPI)
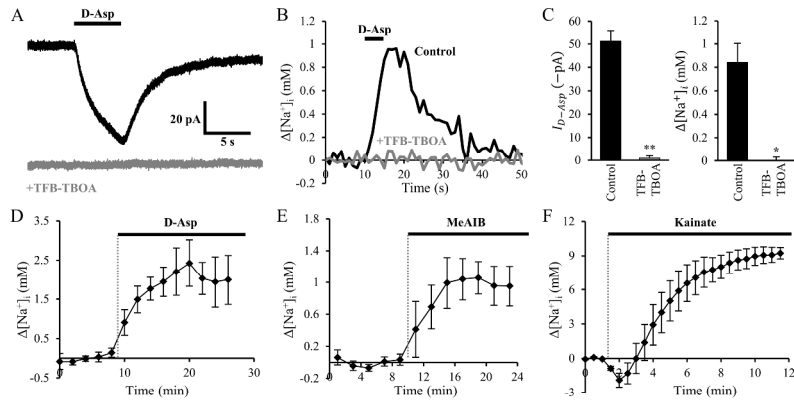
FIGURE 6

FIGURE 6: Glutamate receptor and transporter activation increases astrocytic sodium concentration.
Fig. 6
275x397mm (300 x 300 DPI)
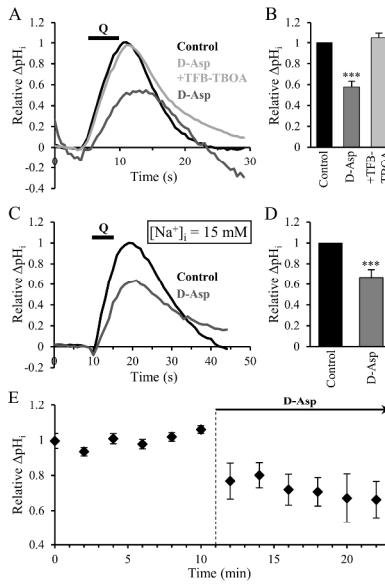
Figure 7

FIGURE 7: Increasing astrocytic $[Na^+]_i$ by EAAT activation reduces SNAT3 mediated glutamine influx.
Fig. 7
275x397mm (300 x 300 DPI)
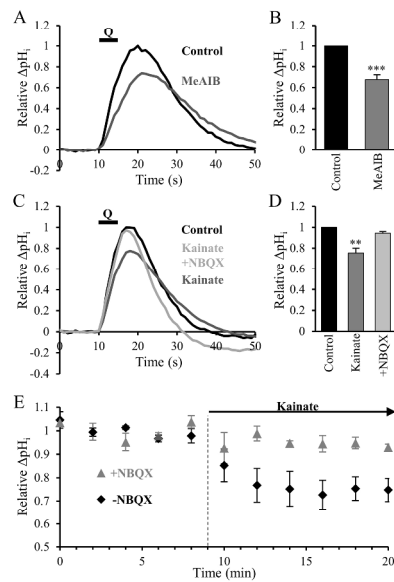
Figure 8

FIGURE 8: Increasing astrocytic $[Na^+]_i$ by SA and AMPA receptor activation reduces SNAT3 mediated glutamine influx.
Fig. 8
275x397mm (300 x 300 DPI)
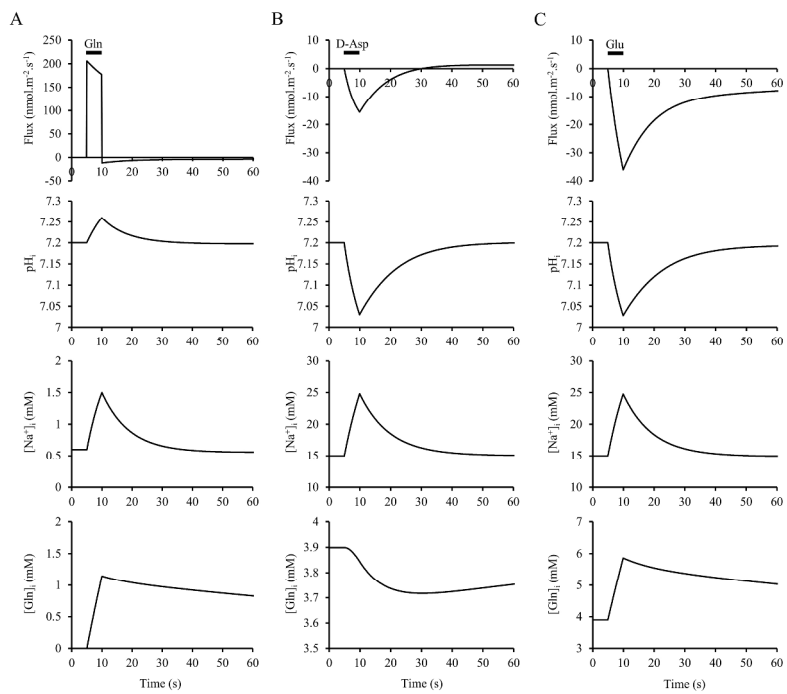
FIGURE 9

FIGURE 9: Model of SNAT3 mediated fluxes shows glutamine release upon EAAT activation.
Fig. 9
275x397mm (300 x 300 DPI)
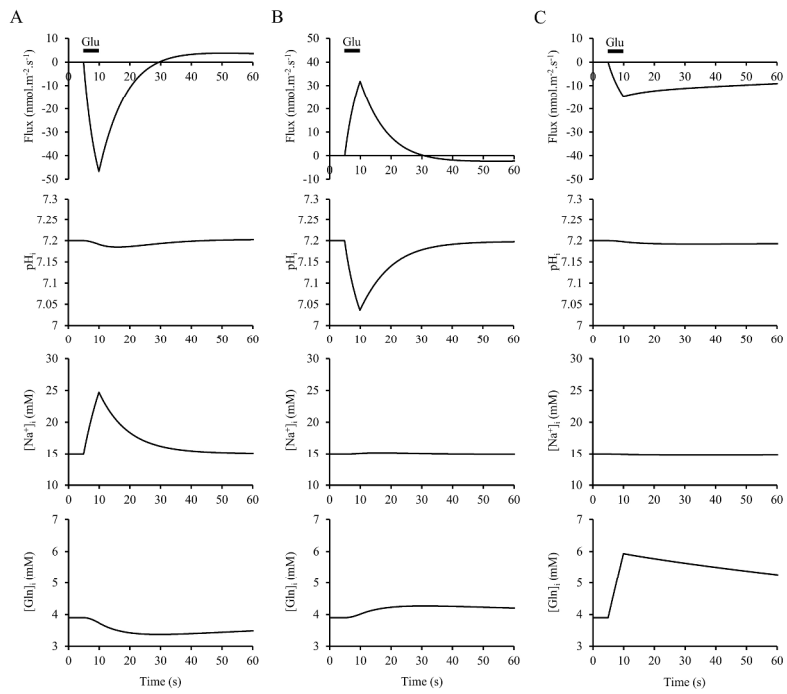
FIGURE 10

FIGURE 10: Glutamine efflux is driven mainly by changes in $[Na^+]_i$.
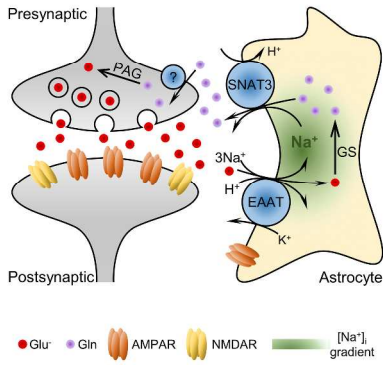Fig. 10
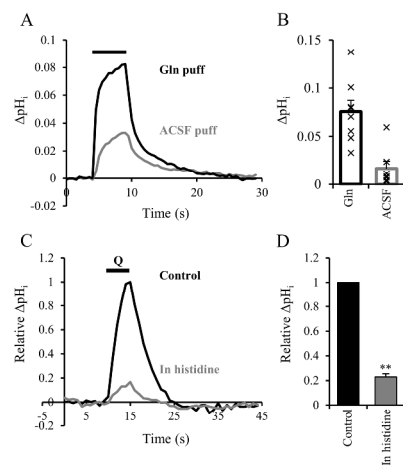275x397mm (300 x 300 DPI)

FIGURE 11

FIGURE 11: SNAT3 mediated glutamine efflux is stimulated by $[Na^+]_i$ and forms part of the glutamate-glutamine cycle.
Fig. 11
275x397mm (300 x 300 DPI)

Supplementary figure 1

SUPPLEMENTARY FIGURE 1. pH responses to puff-application of substrates in bicarbonate buffered external solution contain artefacts.
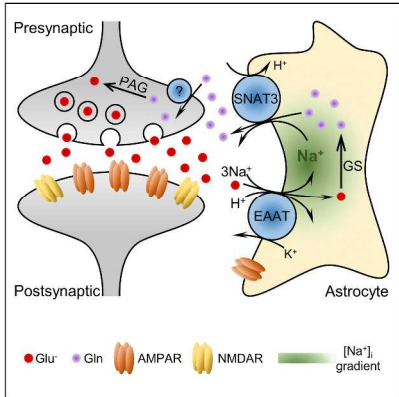Supplementary Fig. 1
275x397mm (300 x 300 DPI)

Table of Contents Image

Table of Contents Image

275x397mm (300 x 300 DPI)